JTTEE5 18:708–713
DOI: 10.1007/s11666-009-9367-5
1059-9630/$19.00 © ASM International

Technical Note

Bond Strength of Multicomponent White Cast Iron Coatings Applied by HVOF Thermal Spray Process

Ossimar Maranho, Daniel Rodrigues, Mario Boccalini, and Amilton Sinatora

(Submitted June 1, 2009; in revised form June 25, 2009)

Multicomponent white cast iron is a new alloy that belongs to system Fe-C-Cr-W-Mo-V, and because of its excellent wear resistance it is used in the manufacture of hot rolling mills rolls. To date, this alloy has been processed by casting, powder metallurgy, and spray forming. The high-velocity oxyfuel process is now also considered for the manufacture of components with this alloy. The effects of substrate, preheating temperature, and coating thickness on bond strength of coatings have been determined. Substrates of AISI 1020 steel and of cast iron with preheating of 150 °C and at room temperature were used to apply coatings with 200 and 400 μm nominal thickness. The bond strength of coatings was measured with the pull-off test method and the failure mode by scanning electron microscopic analysis. Coatings with thickness of 200 μm and applied on substrates of AISI 1020 steel with preheating presented bond strength of 87 ± 4 MPa.

Keywords bond strength, HVOF, multicomponent white cast iron, preheating, thermal spraying

1. Introduction

Multicomponent white cast iron is a new alloy that belongs to the Fe-C-Cr-W-Mo-V system. Since the 1980s it has been used in the manufacture of hot rolling mills rolls for the steel industry and grinding bodies for the mining and cement industry (Ref 1). Characteristics of such alloy include good wear resistance and the capacity to retain a high level of hardness at high temperatures (Ref 2). AISI M2 steel also presents the same characteristics but a lower volumetric fraction of eutectic carbides. Therefore, for this work the standard AISI M2 steel was used in the alloy with added carbon and vanadium to increase the volumetric fraction of the eutectic carbides (Ref 3).

To date, casting, powder metallurgy, and spray forming have been used for the manufacture of components with multicomponent white cast iron alloy (Ref 4, 5). Now, high-velocity oxyfuel (HVOF) thermal spray is being considered as an alternative for the manufacture of components using this alloy. This process is considered here because it is also used for deposition of wear-, corrosion-, or temperature-resistant barriers coatings in a number of industrial applications (Ref 6-9). In the HVOF thermal spray process, the gaseous products of hydrocarbon combustion flow through a supersonic nozzle to form a hot, high-speed jet. This gas flow accelerates and heats injected metal particles to high velocities and temperatures. These particles, upon striking the surface of a substrate, form a strong, dense coating having desirable properties. The flame temperature can be of the order of 3100 °C and the particle velocity of the order of 750 m/s (Ref 7, 8, 10). In the HVOF thermal spray process, the particles present smaller temperature and greater velocity when compared with other thermal spray process. These conditions are responsible for smaller, thermally activated transformation of the particles. Then, materials applied by this process are less inclined to undergo microstructure transformation, which can modify the properties in some materials, for instance, the decarburization of hard metal coatings (Ref 11). Moreover, coatings with porosity of 2% and bond strength of 70 MPa are obtained by HVOF due to high velocity of particles (Ref 8, 9).

Therefore, the HVOF thermal spray process is the most suited to applying multicomponent white cast iron coatings. In fact, in a previous paper by the author, porosity of 0.9% and hardness of 766 HV0.3 were obtained in multicomponent white cast iron coatings applied by HVOF (Ref 12). However, these values demonstrated the possibility of applying coatings with quality, but not the capacity of these coatings to adhere to the substrate with sufficient bond strength to support the work solicitations.

The objective of present work is to determine the influence of the substrate, preheating temperature, and coating thickness on bond strength of multicomponent white cast iron coatings applied by HVOF thermal spray process.

Ossimar Maranho, Federal University of Technology - Paraná, Curitiba, Brazil; **Daniel Rodrigues** and **Mario Boccalini**, Institute for Technological Research, São Paulo, Brazil; and **Amilton Sinatora**, University of São Paulo, São Paulo, Brazil. Contact e-mail: maranho@utfpr.edu.br.

2. Experimentation

High-velocity oxyfuel spraying was carried out using METCO Diamond Jet HVOF gun with DJ 2701 air cap (Sulzer Metco Inc., Westbury, NY). During spraying, the propane flow rate, oxygen flow rate, and compressed air flow rate were fixed at 52, 171, and 346 L/min, respectively. These gas flows have been used to obtain oxygen-to-propane volume ratio of 4.6 that is lower than the stoichiometric rate of the flame, therefore a carburizing flame. This flame can minimize the particle oxidation during spraying and, consequently, the carbon evaporation as CO or CO_2. Spray distance was kept at 200 mm. Prior to deposition, samples of 25.4 mm diameter and 25.4 mm height have been degreased and, subsequently, grit blasted using No. 24 alumina grit. This abrasive has been sufficient to obtain surface roughness of about R_a 6.0 μm in substrates of AISI 1020 steel and of hypoeutectic alloy of multicomponent white cast iron. Moreover, preheating the substrate was carried out using the thermal spray gun, and it was measured by a contact pyrometer with type K (NiCr/NiAl) thermocouple.

The powder of hypereutectic alloy of multicomponent white cast iron with chemical composition (wt.%) of 2.5 C, 4 Cr, 4 Mo, 2 W, and 8 V was obtained by the gas atomization process. It was used as the starting spray powder with a particle size range between 20 and 45 μm. Characterization of powder morphology and powder phases together with macrostructure of cross sections and porosity of deposited coatings were conducted in previous work published by the author (Ref 12).

Coatings were deposited in accordance with spray parameters described in Table 1. Coating 1 was applied on AISI 1020 steel substrate (AC in Table 1) without preheating, and coating 2 was deposited on same substrate with preheating of 150 °C, both with nominal thickness of 200 μm. In the same way, coatings 3 and 4 were deposited on hypoeutectic alloy of multicomponent white cast iron substrate (FF in Table 1) at room temperature and preheating at 150 °C, respectively. On the other hand, coatings 5 and 6 were also deposited on AISI 1020 steel substrate but now with nominal thickness of 400 μm, coating 5 without preheating and coating 6 with preheating at 150 °C. Moreover, coatings were deposited on hypoeutectic multicomponent white cast iron substrate with the same thickness and preheating, which are described in coatings 7 and 8, respectively.

Table 1 Spray parameters used for coating deposition on samples for pull-off test

Coating	Substrate	Thickness, μm	Preheating temperature, °C
1	AC	200	Room
2	AC	200	150
3	FF	200	Room
4	FF	200	150
5	AC	400	Room
6	AC	400	150
7	FF	400	Room
8	FF	400	150

Standard specimens used in the pull-off test have been made of AISI 1020 steel that were bonded together using HTK Hamburg (Hamburg, Germany) epoxy designed as Ultrabond 100 and mounted in a self-aligning loading device. The tensile load was applied using a Universal Instron tension testing machine (Instron Ltd, High Wycombe, Bucks). Following the procedure delineated in ASTM standard C 633 (Ref 13), the bond strength (tensile strength) of the epoxy (without the sprayed coating) was calculated using the ultimate force divided by the cross-sectional area. A value of 98 ± 2 MPa was determined as an average value of five tests. The coated samples have been glued by using epoxy and aligned in a self-aligning device until the bonding agent is cured at temperature of 150 °C for 80 min. Five samples were tested for each condition, and the average value is reported. ASTM C 633 standard recommends that the thickness of coatings must be greater than 380 μm to prevent epoxy penetration. Therefore, in this work the samples coated with thickness of 400 μm are in accord with ASTM C 633 standard. However, samples coated with thickness of 200 μm are thinner than that determined by ASTM C 633 standard. On the other hand, other authors have demonstrated that there is no penetration of adhesive into coatings with thickness of 200 μm (Ref 14, 15). Thus, the fracture surface of coatings was analyzed by scanning electron microscopy (SEM) (backscattering image) to determine the epoxy penetration. In the same way, SEM and optical microscopy were used to qualify the failure mode, which occurred as result of the tensile test. The mode of coating failure will be either adhesive or cohesive. An adhesive failure occurs when the entire coating separates from the substrate. A fracture occurring entirely within the coating is of a cohesive nature. Moreover, failure can occur in the epoxy that indicates the minimum tension that the coating supports. Although inaccurate, this analysis gives an idea of the minimum tensile bond strength of the coating.

3. Results

3.1 Bond Strength

Table 2 shows the results of the average failure load and predominant failure mode for all the samples, which have been tested using ASTM C 633 standard. Bond strength (Fig. 1) is plotted as a function of preheating

Table 2 Bond strength and predominant failure mode of the coatings

Coating	Bond strength, MPa	Predominant failure mode
1	71 ± 6	Adhesive
2	87 ± 4	Epoxy
3	72 ± 3	Adhesive
4	84 ± 5	Adhesive/epoxy
5	55 ± 6	Adhesive
6	56 ± 3	Adhesive
7	44 ± 5	Adhesive
8	54 ± 5	Adhesive

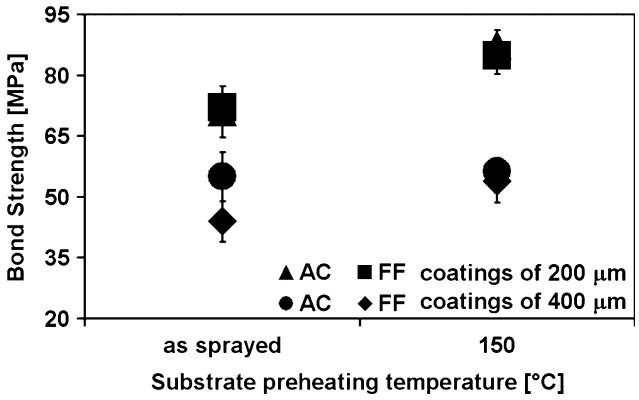

Fig. 1 Measured bond strength vs. substrate preheating temperature for coatings with 200 and 400 µm thickness

temperature for coatings with thicknesses of 200 and 400 µm deposited on AC and FF substrate.

3.1.1 Influence of Substrate Material. The experiments by depositing the coating on the substrate of different materials showed that when the material of the substrate was AISI 1020, the bond strength characteristics of coatings were similar to those of the coatings that were deposited on a hypoeutectic multicomponent white cast iron substrate. Figure 1 shows that the bond strength of coatings with thicknesses of 200 and 400 µm is similar when applied on both substrates, independent of its preheating temperature.

3.1.2 Influence of Coating Thickness. Bond strength of coatings to apply on AC and FF substrate, with thicknesses of 200 and 400 µm, is plotted in Fig. 1. Test results show that the bond strength values are strongly influenced by thickness of coatings. For coatings deposited on AC and FF substrate without preheating, for an increase in coating thickness to 400 µm the average value of bond strength diminishes 22 MPa. In the same way, the average value of bond strength diminishes 30 MPa with the coating thickness increase of 200 to 400 µm for coatings deposited on both substrates with preheating of 150 °C.

3.1.3 Influence of Preheating Temperature. The influence of substrate preheating temperature on bond strength of coatings is shown in Fig. 1 for coatings with thicknesses of 200 and 400 µm. The bond strength presented dissimilar behavior with the increase of substrate preheating when the coatings were deposited with different thickness. For coatings with thickness of 200 µm (Fig. 1), it was observed that increasing the preheating temperature increased the bond strength of the coatings. On the other hand, the preheating temperature did not have the same effect on bond strength of the coatings with thickness of 400 µm (Fig. 1).

3.2 Morphology and Failure Analysis

The fracture surface of every sample and counterpart, corresponding to each group of spray parameters summarized in Table 1, has been characterized using optical and scanning electron microscopy. The predominant mode

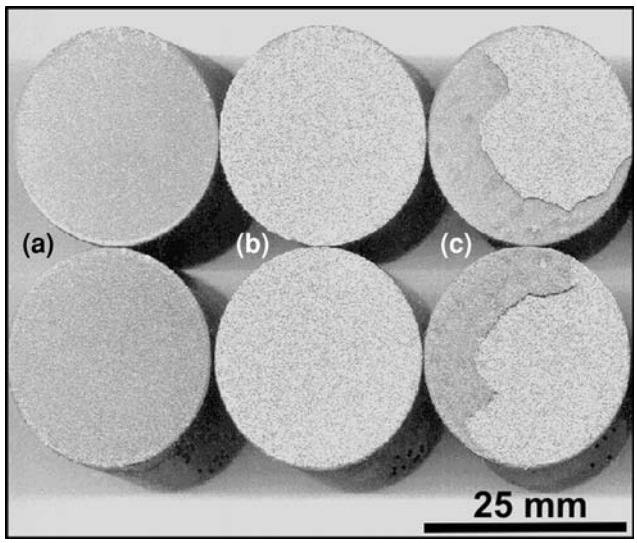

Fig. 2 Example of the fracture surface with top view of samples (coated side) and of counterpart (epoxy side). (a) Failure in the epoxy. (b) Adhesive failure. (c) Mixed failure

of failure was determined by macroscopic image analysis of the fracture surface of these samples. The results are presented in Table 2. Figure 2 shows one sample (coated side) and its counterpart (epoxy side) for each failure mode. The total failure in the epoxy, indicated as (a) in Fig. 2, was detected only in coatings with 200 µm deposited on preheated AISI 1020 substrate. In the same way, mixed failure mode [sample (c) in the Fig. 2] was only detected in the coating with 200 µm deposited on preheated multicomponent white cast iron substrate. Figure 2 also shows, indicated as (b), the adhesive failure mode that occurs in all other coatings.

Analysis using optical microscopy does not identify exactly with precision the place of failure. For this reason, SEM has been used to determine exactly the location of failure, that is, if the adhesive failure occurred in coating/substrate interface or in interior of the coating and if epoxy failure would have been in the interior of coating. Surface with epoxy failure is presented with greater magnification in Fig. 3(a). It is possible to observe that the surface presents dark coloration in all its extension beyond some white points. Figure 3(b) shows that the observed white points are regions where the failure in the epoxy occurs and that the dark regions are the adhesive layer. In the same way, Fig. 4(a) also shows the surface where adhesive failure occurs. Unlike failure in the epoxy, this surface presents white coloration in all its extension with some black points. Analysis with greater magnification of the black points (Fig. 4b) allows the observation that these regions are constituted of aluminum oxide particles, which have been encrusted during grit blasting prior to deposition of coating. Therefore, SEM analyses performed on the surface of the fracture corroborate the existence of adhesive failure as well as failure in epoxy detected when using optical microscopy. Moreover, this analysis shows that there is no penetration of epoxy into the coatings;

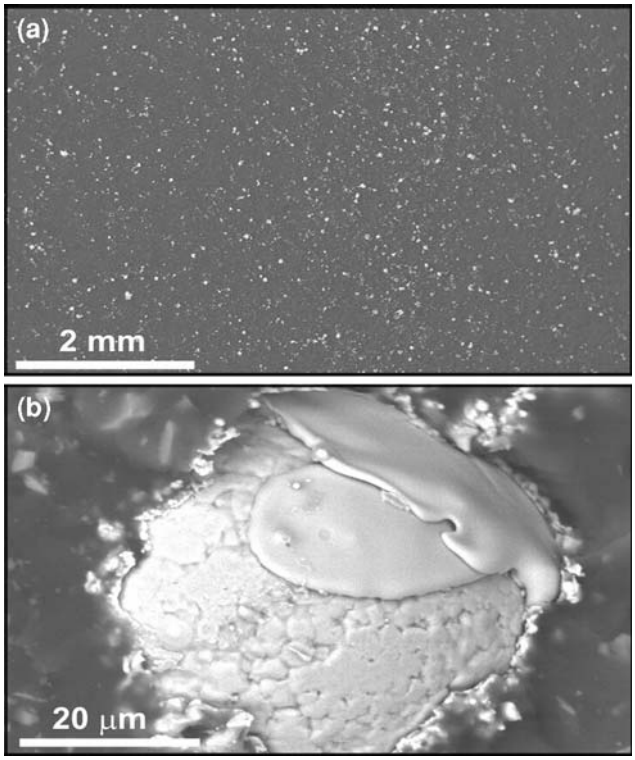

Fig. 3 Scanning electron micrographs of the surface with failure in the epoxy. (a) General view. (b) Detail of white regions (backscattering image)

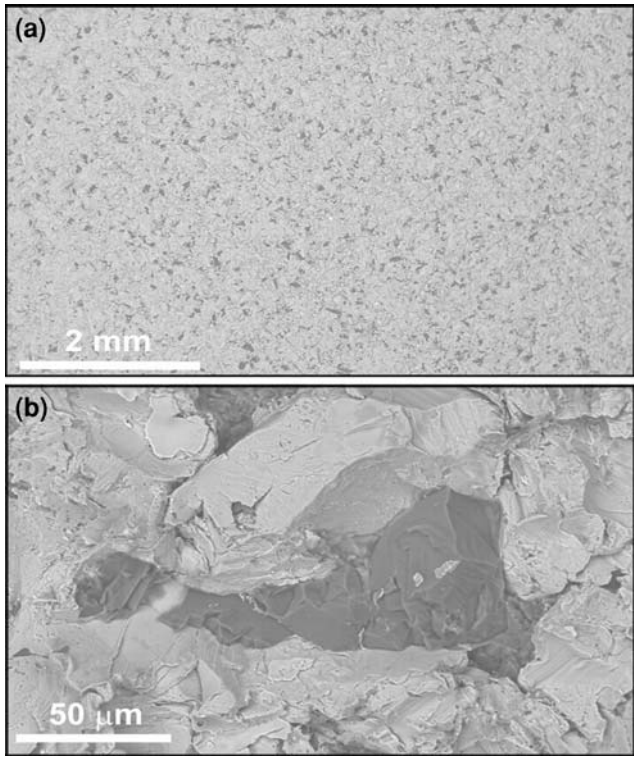

Fig. 4 Scanning electron micrographs of the surface with adhesive failure. (a) General view. (b) Details of dark regions (backscattering image)

therefore, the bond strength of coatings with 200 μm was not influenced by epoxy. In the epoxy failure mode, there is no influence of porosity in the results because the failures started in the glue, as shown in Fig. 3(b). On the other hand, in the adhesive failure mode if the adhesive had penetrated into the coating it would be detected by the analysis of the sample surface. However, Fig. 4(b) shows that the black points are particles of abrasive and not epoxy.

Scanning electron microscopic analysis was also used to characterize the mixed failure mode indicated as (c) in Fig. 2. Figure 5(a) shows with greater magnification the mixed failure mode, which started with adhesive failure (region I) and failed by separation through the epoxy (region II). The transition between these regions is abrupt, and there is no cohesive failure, as shown in Fig. 5(b). In the location of change between adhesive failure and epoxy failure the coating was fractured. The coating fracture occurred in the following locations: interface between lamellas, interface between lamellas and unmelted particles, and inside of lamellas. These locations are labeled in Fig. 5(b) as g, h, and f, respectively.

4. Discussion

The bond strength of the coating is mainly changed as a result of residual stresses generated in deposition process (Ref 16-19). The residual stresses are caused by shrinkage of the particles sprayed after solidification (primary cooling process) or differences between the thermal expansion coefficients of the coating and of the substrate (secondary cooling process). The primary cooling process is by cooling the particles from the melting temperature to the temperature reached by the substrate during deposition process. The stresses generated by this process are called deposition, intrinsic, or quenching stresses (Ref 18). So, these stresses are dependents of modulus of elasticity and thermal expansion coefficient of the material sprayed and of the difference of temperature between substrate and coating (Ref 19). On the other hand, the secondary cooling process is induced by the mismatch of thermal shrinkage during cooling from the process temperature (average temperature reached by the coating/substrate system after deposition) to room temperature. In this case, the residual stresses are dependent on the thermal expansion coefficient of the substrate and coating, on the melting temperature of the particles, and on temperature of the substrate (Ref 19). In this work, the coating has been applied on substrates with same roughness and temperature (as sprayed or 150 °C) then only the thermal expansion coefficient and melting temperature of the particles would be responsible for modifying the residual stresses. As demonstrated in the results, no variation occurred in the bond strength of the coatings with 200 and 400 μm thick applied on two

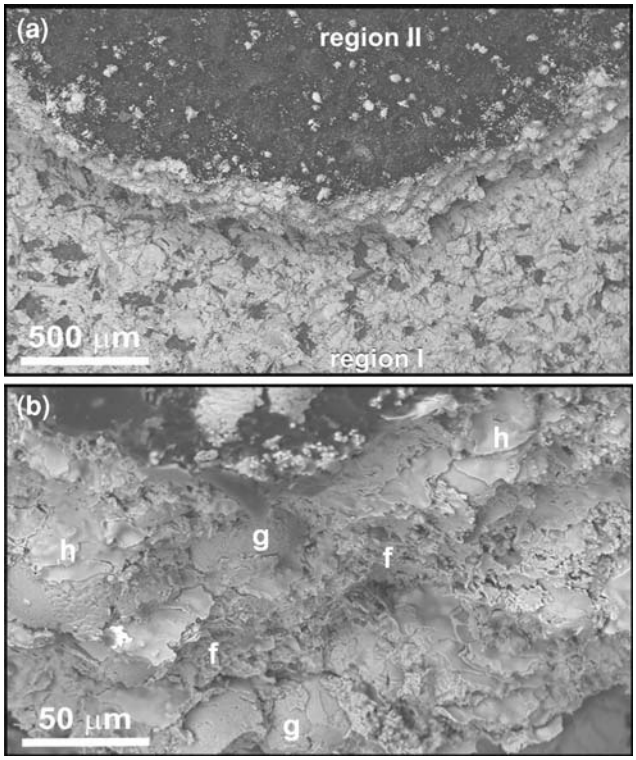

Fig. 5 Scanning electron micrographs of the surface with mixed failure. (a) General view. (b) Details of the region of coating fracture (backscattering image)

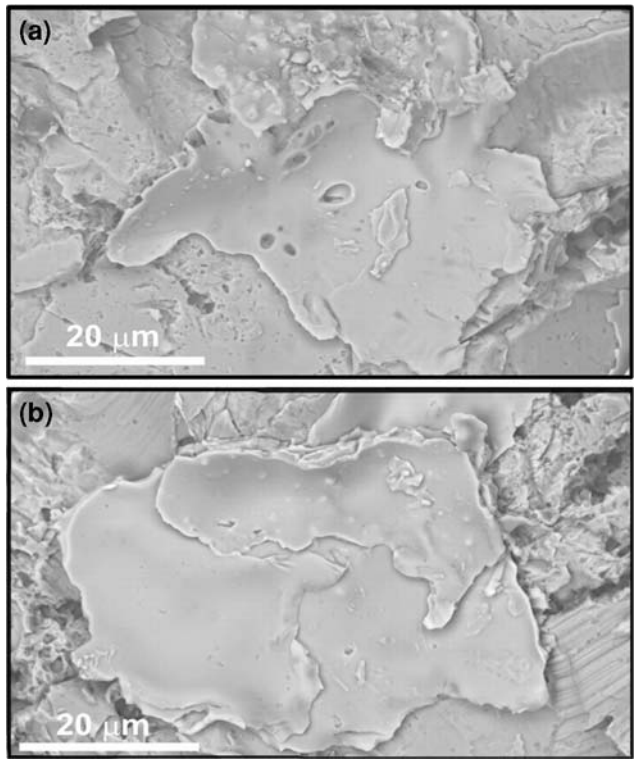

Fig. 6 Scanning electron micrographs of splats morphology. Particles were sprayed on (a) substrates without preheating and (b) substrates with preheating of 150 °C (backscattering image)

substrates. Then, although it has not been measured, the difference between the properties of substrate materials has been insufficient to cause a change in the level of stresses and, consequently, the bond strength of the coatings.

On the other hand, preheating the substrate may significantly improve the bond strength of coatings with thickness of 200 μm, but did not change the bond strength of coatings with thickness of 400 μm. This behavior can be mainly attributed to the predominance of different mechanisms in the formation of residual stresses of coatings with 200 and 400 μm thickness. For all coatings, the increase of the substrate temperature produced a change in splat shape. In the substrates without preheating, Fig. 6(a), the splat presents irregular contours and the presence of pores. On the other hand, with the preheating temperature increased up to 150 °C (see Fig. 6b), the splats present more spherical contours and without pores. The more continuous and homogeneous splats have a bigger area of contact with the substrate, therefore more heat transfer (Ref 20-22). Besides that, this format of splats increases bond strength of the coatings by improving the mechanical interlocking and diffusion mechanisms (Ref 23, 24). Together with the change in the morphology of splats, preheating also modifies the levels of stresses generated in thermal spray process (Ref 16, 17). The smaller level of residual stress for the substrate with the greater preheating temperature results mainly from the decrease of difference of temperature between the sprayed materials and the substrate. Therefore, the bond strength of the coating increased from 70 up to 85 MPa with the increase of the preheating temperature at 150 °C for both substrates, with coating thickness of 200 μm.

The preheating temperature did not cause the same effect on coatings applied with thickness of 400 μm. In this case, the bond strength has been equal for coatings applied on substrates with a preheating temperature of 150 °C and for those kept at room temperature. It was demonstrated that with increasing the coating thickness the level of stresses increased mainly by the effect of the secondary cooling process (Ref 25). Moreover, preheating has more influence in the deposition of first layers because for the next layers a decrease of the difference of temperature occurs between the coating and substrate (Ref 26). Therefore, the preheating temperature has not been enough to minimize the stresses generated in secondary cooling of coatings applied with thickness of 400 μm.

The hypotheses about the influence of residual stresses on bond strength are in accordance with the literature, but they need experimental evidence. Future work will be carried out to measure the involved stresses in deposition process of multicomponent white cast iron coatings.

5. Conclusions

The effects of substrate material, substrate preheating temperature, and thickness of coatings on bond strength of

hypereutectic multicomponent white cast iron coatings deposited by HVOF thermal spray were investigated using the pull of test delineated in ASTM standard C 633. The following conclusions have been obtained using the set of parameters of this job. Substrate material presented no influence on bond strength of the coating when used with preheating or at room temperature. Results showed that bond strength is strongly influenced by the coating thickness. Coatings with greater thickness had lower bond strength. Preheating temperature has produced different behaviors on coatings applied with 200 and 400 μm thickness. Bond strength of a coating with a thickness of 400 μm presented no change with the preheating temperature. However, for coatings with thickness of 200 μm, the increase of the preheating temperature increased the bond strength of the coating. Coatings with thickness of 200 μm and applied on substrates of AISI 1020 steel with preheating presented bond strength of 87 ± 4 MPa.

References

1. H.Q. Wu, N. Sasaguri, Y. Matsubara, and M. Hashimoto, Solidification of Multi-Alloyed White Cast Iron: Type and Morphology of Carbides, *Trans. Am. Fish. Soc.*, 1996, **140**, p 103-108
2. M. Boccalini, Jr., and H. Goldenstein, Solidification of High Speed Steels, *Int. Mater. Rev.*, 2001, **46**(2), p 92-115
3. Y. Matsubara and M. Hashimoto, Metallurgical Aspect of Multi-Component White Cast Irons for Hot Rolling Mill Roll, *Proceedings of the 44th MWSP Conference,* 2002, Vol XL, p 23-31
4. A.H. Kasama, A.J. Mourisco, C.S. Kiminami, W.J. Bota Fo, and C. Bolfarini, Microstructure and Wear Resistance of Spray Formed High Chromium White Cast Iron, *Mater. Sci. Eng. A*, 2004, **375-377**, p 589-594
5. T. Koseki, K. Ichino, and Y. Kataoka, Development of Centrifugal Cast Roll with High Wear Resistance for Finishing Stands of Hot Strip Mill, *Kawasaki Steel Tech. Rep.*, 1997, **37**, p 13-18
6. E. Lugscheider, H. Eschnauer, U. Muller, and T.H. Weber, Quo Vadis, Thermal Spray Technology, *Powder Met. Int.*, 1991, **1**(23), p 33-39
7. R.W. Smith and R. Novak, Advanced and Applications in U.S. Thermal Spray Technology, *Powder Met. Int.*, 1991, **23**(3), p 147-154
8. American Welding Society, *Thermal Spraying Technology*, Miami, 1985, p 184
9. J.R. Davis, Ed., *Handbook of Thermal Spray Technology*, ASM International, Materials Park, OH, 2004, p 338
10. M.L. Thorpe, Thermal Spray Industry in Transition, *Adv. Mater. Processes*, 1993, **5**, p 50-61
11. R. Schwetzke and H. Kreye, Microstructure and Properties of Tungsten Carbide Coatings Sprayed with Various High-Velocity Oxygen Fuel Spray Systems, *J. Therm. Spray Technol.*, 1999, **8**(3), p 433-439
12. O. Maranho, D. Rodrigues, M. Boccalini, Jr., and A. Sinatora, Influence of Parameters of the HVOF Thermal Spray Process on the Properties of Multicomponent White Cast Iron Coatings, *Surf. Coat. Technol.*, 2008, **202**, p 3494-3500
13. "Test Method for Adhesion or Cohesive Strength of Flame Sprayed Coatings," C 633, ASTM, p 754-760
14. L. Pawlowski, *The Science and Engineering of Thermal Spray Coatings*, Wiley, New York, 1995, p 184
15. E. Bardal, P. Molde, and T.G. Eggen, Arc and Flame Sprayed Aluminium and Zinc Coatings on Mild Steel: Bond Strength, Surface Roughness, Structure and Hardness, *Br. Corros. J.*, 1973, **8**, p 15-19
16. T.C. Totemeyer and J.K. Wright, Residual Stress Determination in Thermally Sprayed Coatings—A Comparison of Curvature Models and X-ray, *Surf. Coat. Technol.*, 2006, **200**, p 3955-3962
17. M.S.J. Hashmi, C. Pappalettere, and F. Ventola, Residual Stresses in Structures Coated by High Velocity Oxy-Fuel Technique, *J. Mater. Process. Technol*, 1998, **75**, p 81-86
18. T.W. Clyne and S.C. Gill, Residual Stresses in Thermal Spray Coatings and Their Effect on Interfacial Adhesion: A Review of Recent Work, *J. Therm. Spray Technol.*, 1996, **5**(4), p 401-418
19. C. Godoy, E.A. Souza, M.M. Lima, and J.C.A. Batista, Correlation Between Stresses and Adhesion of Plasma Sprayed Coatings: Effects of a Post-Annealing Treatment, *Thin Solid Films*, 2002, **420-421,** p 438-445
20. M. Vardelle, A. Vardelle, A.C. Leger, P. Fauchais, and D. Gobin, Influence of Particle Parameters at Impact on Splat Formation and Solidification in Plasma Spraying Processes, *J. Therm. Spray Technol.*, 1994, **4**(1), p 50-58
21. M. Parco, L. Zhao, J. Zwick, K. Bobzin, and E. Lugscheider, Investigation of Particle Flattening Behaviour and Bonding Mechanisms of APS Sprayed Coatings on Magnesium Alloys, *Surf. Coat. Technol.*, 2007, **201**, p 6290-6296
22. S. Sampath and X. Jiang, Splat Formation and Microstructure Development During Plasma Spraying: Deposition Temperature Effects, *Mater. Sci. Eng. A*, 2001, **304-306**, p 144-150
23. V. Pershin, M. Lufitha, S. Chandra, and J. Mostaghimi, Effect of Substrate Temperature on Adhesion Strength of Plasma-Sprayed Nickel Coatings, *J. Therm. Spray Technol.*, 2003, **12**(3), p 370-376
24. L. Li, X.Y. Wang, G. Wei, A. Vaidya, H. Zhang, and S. Sampath, Substrate Melting During Thermal Spray Splat Quenching, *Thin Solid Films*, 2004, **468**, p 113-119
25. J. Stokes and L. Looney, Residual Stress in HVOF Thermally Sprayed Thick Deposits, *Surf. Coat. Technol.*, 2004, **177-178**, p 18-23
26. M. Mellali, P. Fauchais, and A. Grimaud, Influence of Substrate Roughness and Temperature on the Adhesion/Cohesion of Alumina Coatings, *Surf. Coat. Technol.*, 1996, **81**, p 275-286